Supplemental Information

A pyrophosphate-activated nanochannel inspired by TRP ion channel

Fei Zhu, Guanxing Yang, Manivannan Kalavathi Dhinakaran, Rui Wang, Miaomiao Song, and Haibing Li*

Key Laboratory of Pesticide and Chemical Biology (CCNU), Ministry of Education, College of Chemistry, Central China Normal University, Wuhan 430079, PR China
E-mail address: lhbing@mail.ccnu.edu.cn

Contents

1. The Synthesis of C4NP

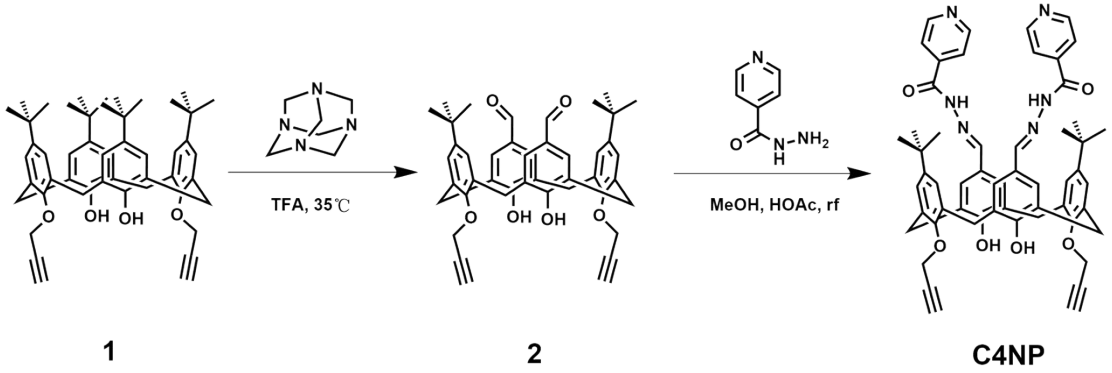

Figure S1. The synthesis route of C4NP.

1.1 Synthesis of compound 2[S1]

2 g Compound **1** (2.76 mmol) and six methyl tetramine 17 g mixture slowly add trifluoroacetic acid (TFA) and nitrogen protection at room temperature under stirring reaction about eight hours, after the reaction, the reaction liquid pour into the left and right sides of crushed ice cool stir constantly, after waiting for ice to melt completely, by several times with chloroform extraction, chloroform layer with saturated sodium chloride water washing to neutral. The chloroform was removed by rotary evaporation and the white product was 0.92g after column chromatography, the yield is 50%. ^{1}H NMR (600 MHz, $CDCl_3$) δ: 9.85 (s, 2H, CHO), 7.77 (s, 2H, ArOH), 7.67 (s, 4H, ArH), 6.79 (s, 4H, ArH), 4.78 (s, 4H, OCH_2), 4.39 (d, J = 13.6 Hz, 4H, $ArCH_2$), 3.50 (d, J = 13.6 Hz, 4H, $ArCH_2$), 2.63 (s, 2H, $CH_2C{\equiv}CH$), 0.93 (s, 18H, Bu^t) ppm. ^{13}C NMR (150 MHz, $CDCl_3$) δ: 191.71, 191.11, 159.11, 149.41, 148.48, 131.48, 130.69, 128.95, 128.60, 126.03, 125.97, 78.08, 64.57, 63.47, 34.07, 31.88, 31.11, 30.89 ppm.

1.2 Synthesis of C4NP

In the double-mouthed flask, isoniazid compound (0.01g, 0.68 mmol) and Compound **2** (0.2g, 0.29 mmol) was added, 20 mL anhydrous methanol was added. The mixture was stirred and refluxed under the catalysis of acetic acid, Compound **2** was

gradually dissolved. The solution was clarified and then gradually turned yellow, followed by gradual precipitation of yellow solids, cooling and filtration. A small amount of methanol was washed for three times to obtain the yellow solids 0.15g, 60% yield. ^{1}H NMR (600 MHz, DMSO) δ: 8.78 (s, 4H, PyH), 8.33 (s, 2H, HC=N), 8.26 (s, 1H, ArOH), 7.83 (s, 4H, PyH), 7.62 (s, 4H, ArH), 7.09 (s, 4H, ArH), 4.86 (s, 4H, OCH_2), 4.30 (s, 4H, $ArCH_2$), 3.81 (s, 2H, CONH), 3.61 (s, 4H, $ArCH_2$), 1.07 (s, 18H, Bu^t) ppm. ^{13}C NMR (150 MHz, DMSO) δ: 161.25, 150.28, 149.80, 149.59, 147.43, 132.45, 128.73, 128.01, 125.89, 125.18, 121.56, 79.71, 78.96, 63.37, 34.04, 31.37, 30.97 ppm. Calcd for m/z=929.399 ($M+Na^+$), found m/z= 929.399 ($M+Na^+$).

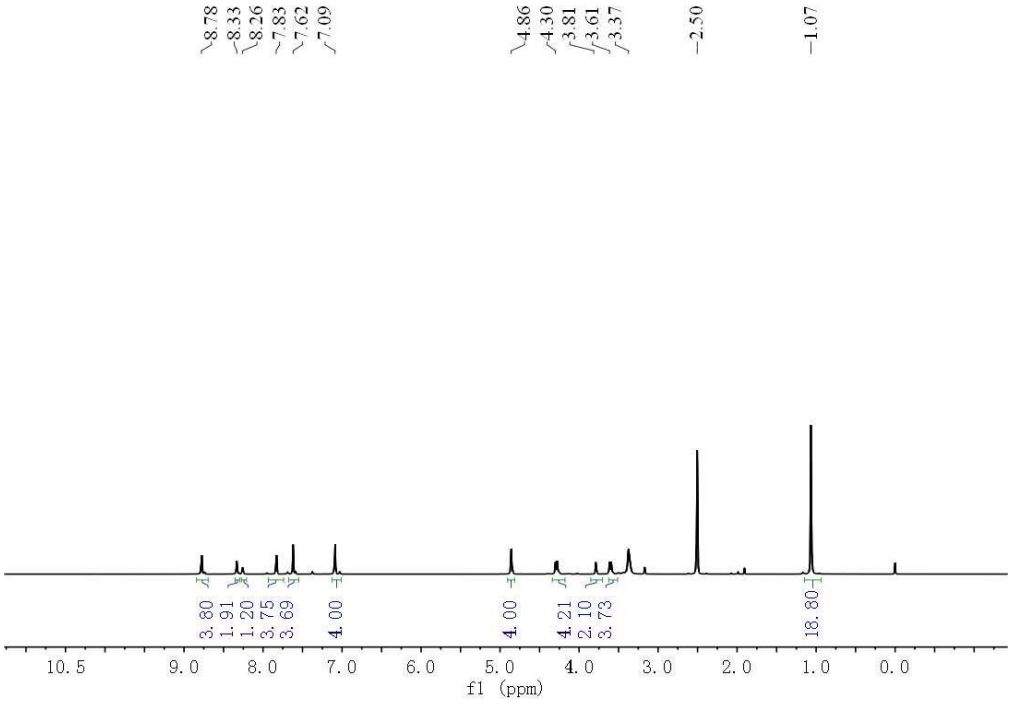

Figure S2. ^{1}H NMR (600M Hz, DMSO-d_6) of C4NP.

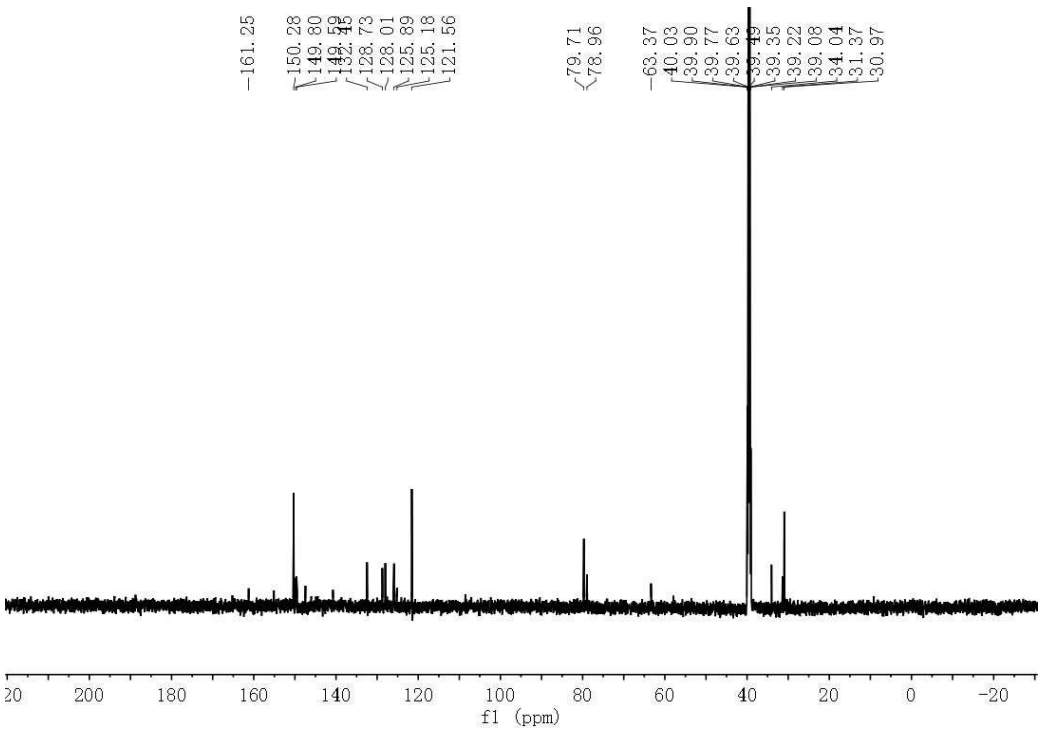

Figure S3. ^{13}C NMR (150M Hz, DMSO-d_6) of C4NP.

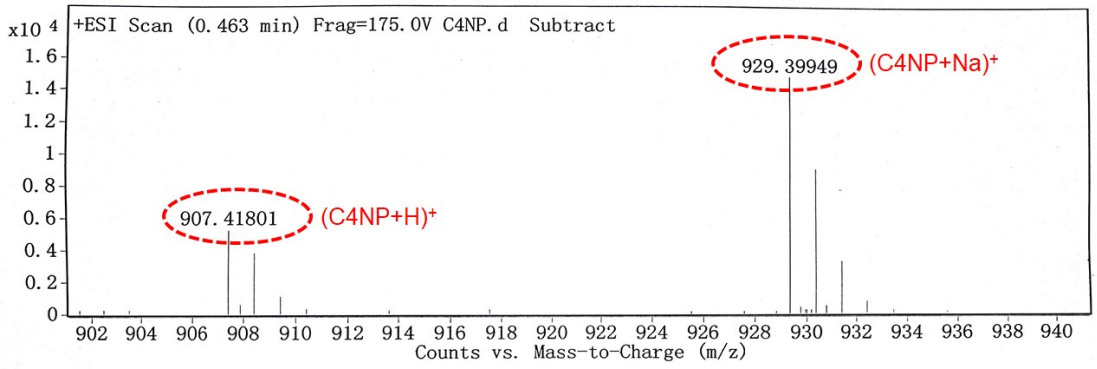

Figure S4. Mass spectrum of C4NP.

2 Characterization of nanochannel pore size

In order to obtain the conical nanochannel, the etching was performed in only one side of the conductivity cell, and the other side of the cell was filled with stopping solution which was able to neutralize the etchant as soon as the pore opened. In this work, the PI membrane was embedded between the two chambers of a conductivity cell at 50℃. One chamber was filled with etching solution (NaClO, 13% available chlorine, pH~12.5), and the other chamber was filled with stopping solution (1 M KI). Then, a voltage of 1 V was applied across the membrane to monitor the current. The etching process was stopped at a desired current value corresponding to a certain tip diameter. The membrane was immersed in distilled water to remove residual salts.

The diameters of large opening (base side) of conical nanochannels were determined by field-emission scanning electron microscopy (FESEM), the tip diameter was estimated by the following relation: [S2]

$$d_{tip} = \frac{4LI}{\pi k(c) UD}$$

L is the length of the nanochannel, which could be approximated to the thickness of the membrane after chemical etching (12 μm); I is the measured ion current; U is the applied voltage; d_{tip} and D is the diameter of tip and base respectively; $k(c)$ is the specific conductivity of the electrolyte. For 1 M KCl solution at 25 ℃, $k(c)$ is 0.11173 Ω^{-1} cm^{-1}.

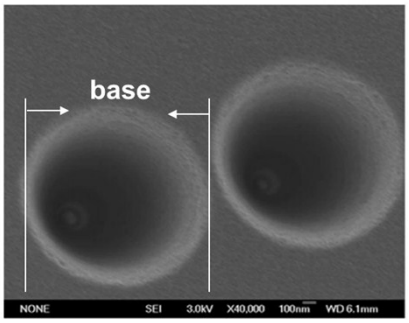

Figure S5. SEM image of the PI membrane. As shown, the base diameter was about 800 nm.

3 Modification of APAM and C4NP

Firstly, the PI film is immersed in the solution that pH 12.5 and the chloride content of sodium hypochlorite is 13% for half an hour at about 50℃, after that, take out and soak in the stop solution of 1M KI for twenty minutes. Then the PI film is rinsed with secondary water and immersed in secondary water overnight. Secondly, the 30 mg EDC and the 6 mg NHS are dissolved in 4mL of 0.1M 4-morpholine ethane sulfonic acid (pH 5.4), oscillating to dissolve completely. The prepared PI film is immersed in the above solution, still standing for 1 hour at room temperature. Then to remove the PI film, After rinsed with secondary water, The film is immersed in 1 mM solution of the APAM to be modified overnight, Lastly, PI film is immersed in 1 mM C4NP solution, 0.87 mg copper sulfate pentahydrate and 1.4 mg sodium ascorbate are dissolved in 10 mL water, the mixed solution that acts as catalytic is added to the above title compound solution, standing overnight. CA test drop is 2 μL, choose five different position to test in a film and get the mean value.

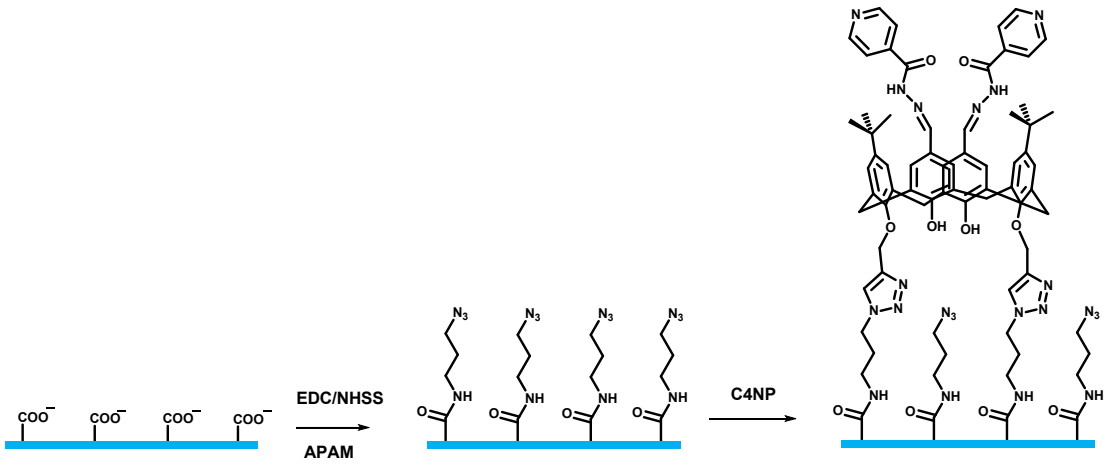

Figure S6. The modification process.

4 XPS of the PI film

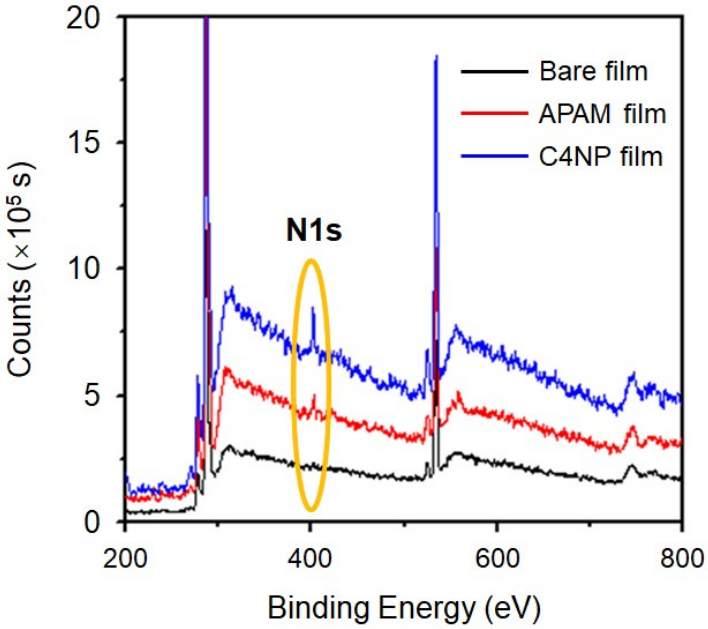

Figure S7. XPS spectrum of the PI film before and after modification.

5 Control experiments of different nanochannels

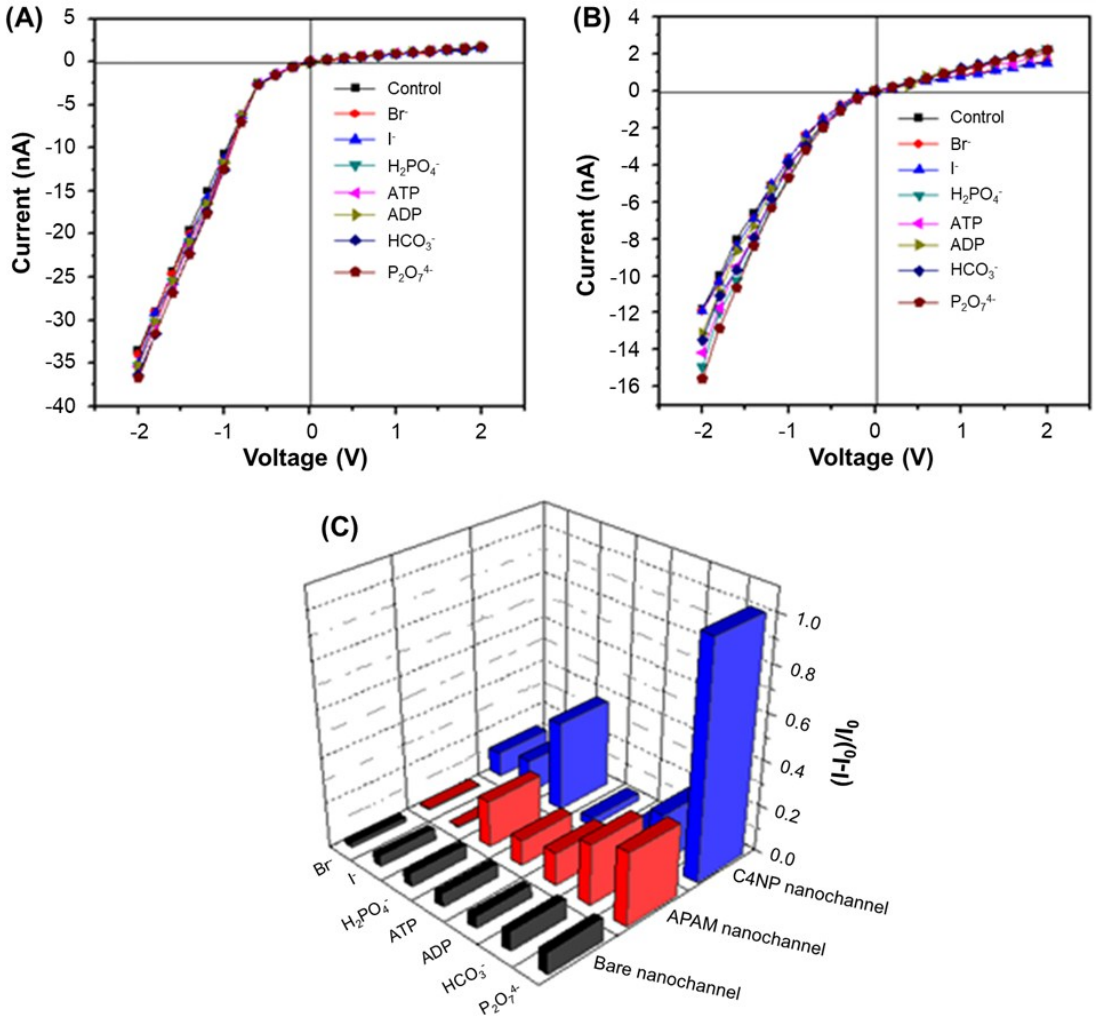

Figure S8. The I-V curves of (A) Bare nanochannel and (B) APAM nanochannel upon adding 1mM various anions. (C) The current change ratio at -2V in three different nanochannels.

6 Determination of the binding constants (*K*) in nanochannel

In previous literature, it was discovered that the Langmuir model provided a perfect fit to the experimental data for nanochannels. [S3, S4] In our work, furthermore, the variation of the rectification ratio ($R_{-/+}$) with increasing concentration of different anions, was similar to the trend of the Langmuir absorption isotherm ($C/R_{-/+} = 1/KR_{max} + C/R_{max}$), where C is the concentration of anion, $R_{-/+}$ is the rectification ratio, and K is the binding strength constant. Consequently, we speculated that it would be possible to describe the binding of anion on the internal surface of the C4NP nanochannel using the Langmuir model.

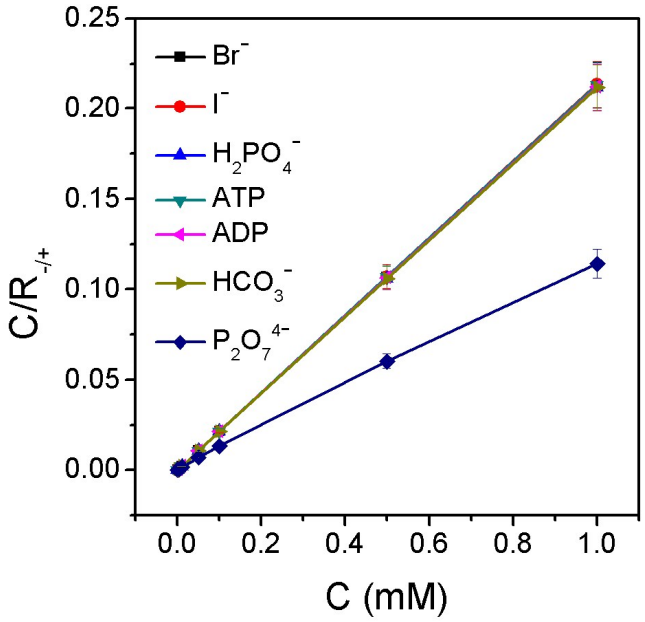

Figure S9. Langmuir isotherm plots of anion adsorption on C4NP nanochannel derived from the data shown in Figure 2D. The degree of rectification ($R_{-/+}$, the ratio of negative to positive current at 2 V) generally increased with increasing initial anion concentrations from 1×10^{-8} to 1×10^{-3} M. The Langmuir model was found to provide a perfect fit to the experimental data. The regression values (R^2) > 0.995 indicate a good fit for both systems. The binding strength constants of various anion in C4NP nanochannel are shown in Table S1.

Table S1. *K* values (binding constants) for the different anions calculated using the Langmuir equation. *K* ($P_2O_7^{4-}$) denotes the *K* of $P_2O_7^{4-}$, and *K* (other anion) is the *K* of any anion except $P_2O_7^{4-}$.

Anion	*K* / M^{-1}	*K* ($P_2O_7^{4-}$) / *K* (other anion)
$P_2O_7^{4-}$	6.86×10^5	/
Br^-	1.64×10^5	4.18
I^-	0.97×10^5	7.06
$H_2PO_4^-$	1.08×10^5	6.34
ATP	0.72×10^5	9.54
ADP	1.13×10^5	6.08
HCO_3^-	1.19×10^5	5.77

7 Determination of the association constants (K_a) in solution

To determine the stoichiometry and association constant (K_a) between C4NP and different anions, ^{1}H NMR titrations were done with solutions which had a constant concentration of C4NP (10 mM) and varying concentrations of anion. Using the nonlinear curve fitting method, the association constant was obtained for each host-guest combination from the following equation: [S5]

$$\Delta\delta = (\Delta\delta_\infty/[G]_0)\left(0.5[H]_0 + 0.5([G]_0 + 1/K_a) - \left(0.5\left([H]_0{}^2 + 2[H]_0\left(\frac{1}{K_a} - [G]_0\right) + \left(\frac{1}{K_a} + [G]_0\right)^2\right)^{0.5}\right)\right)$$

Where $\Delta\delta$ is the chemical shift change of H_1 of tertiary-butyl in C4NP at $[H]_0$, $\Delta\delta_\infty$ is the chemical shift change of H_1 when the C4NP is completely complexed, $[G]_0$ is the fixed initial concentration of the C4NP, and $[H]_0$ is the varying concentrations of anion.

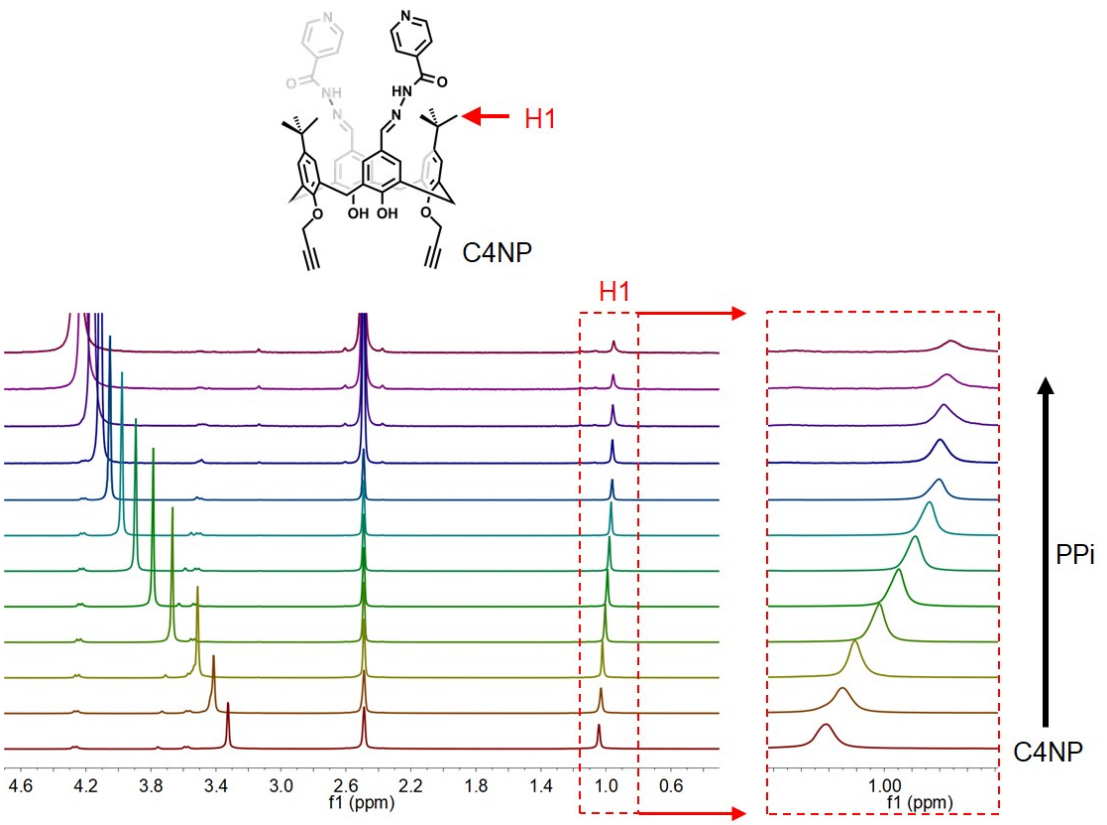

Figure S10. Partial ^{1}H NMR spectra (DMSO-d_6, 298 K, 600 MHz) of C4NP at a concentration of 10 mM upon addition of different concentrations of PPi (0-20 mM, dissolved in D_2O).

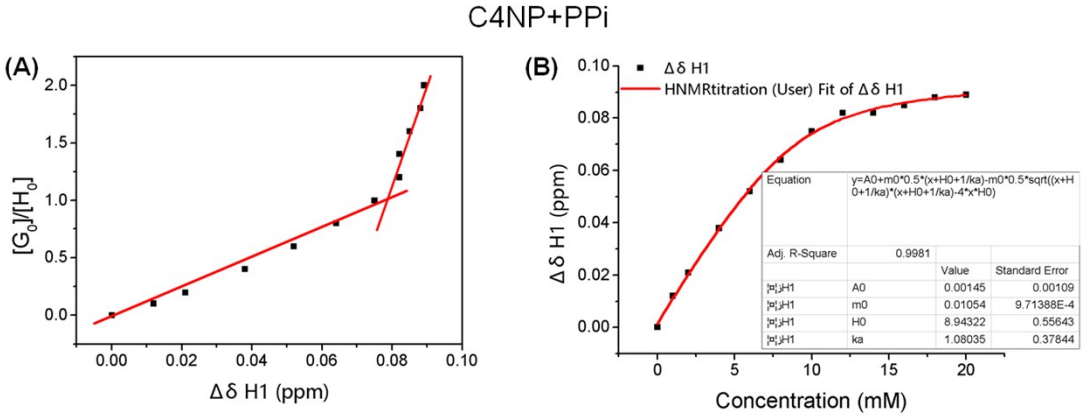

Figure S11. (A) Mole ratio plot for the complexation between C4NP and PPi, indicating a 1:1 stoichiometry; (B) The non-linear curve-fitting (NMR titrations) for the complexation of C4NP with different concentration of PPi. The association constant (K_a) was calculated to be 1.08×10^3 M^{-1}.

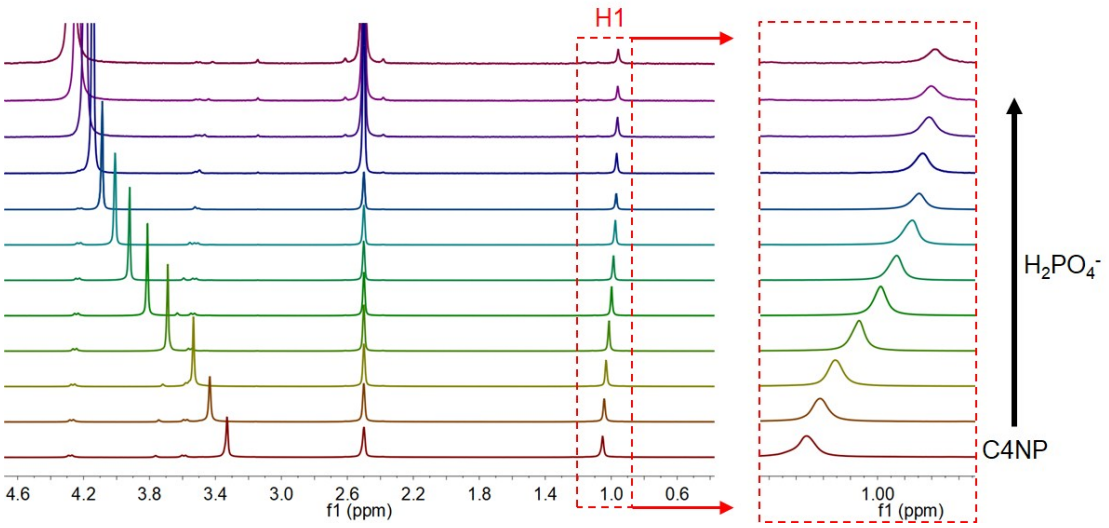

Figure S12. Partial ^{1}H NMR spectra (DMSO-d_6, 298 K, 600 MHz) of C4NP at a concentration of 10 mM upon addition of different concentrations of $H_2PO_4^-$ (0-20 mM, dissolved in D_2O).

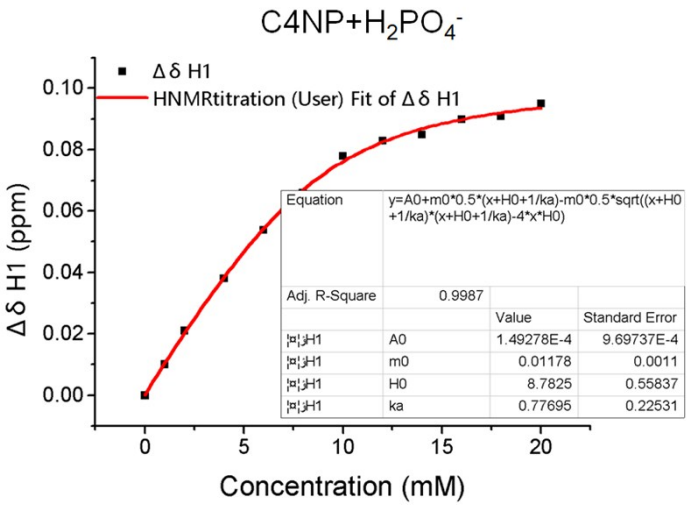

Figure S13. The non-linear curve-fitting (NMR titrations) for the complexation of C4NP with different concentration of $H_2PO_4^-$. The association constant (K_a) was calculated to be 0.78×10^3 M^{-1}.

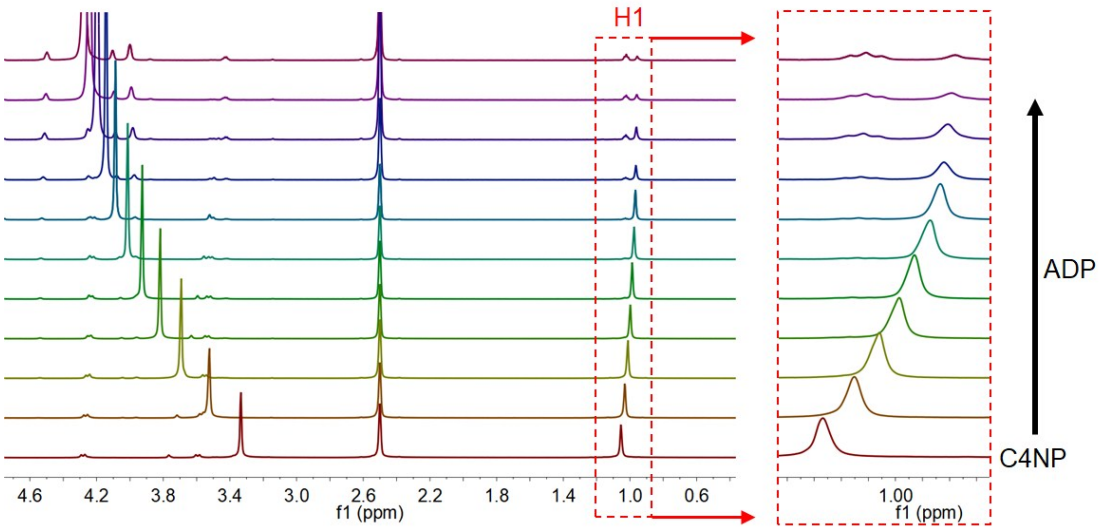

Figure S14. Partial ^{1}H NMR spectra (DMSO-d_6, 298 K, 600 MHz) of C4NP at a concentration of 10 mM upon addition of different concentrations of ADP (0-20 mM, dissolved in D_2O).

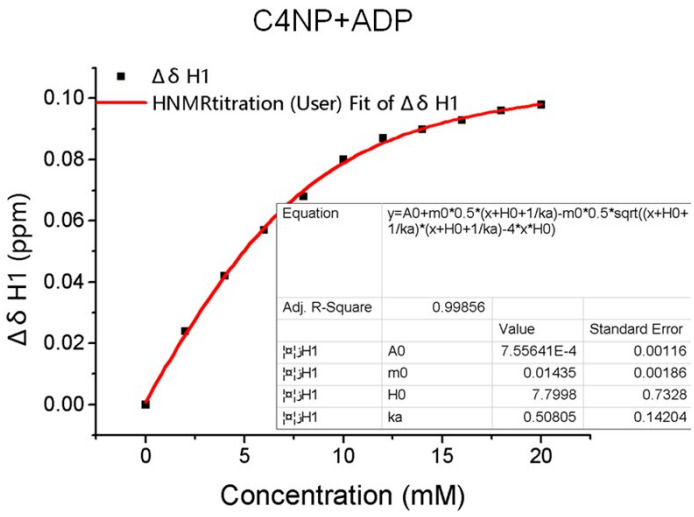

Figure S15. The non-linear curve-fitting (NMR titrations) for the complexation of C4NP with different concentration of ADP. The association constant (K_a) was calculated to be 0.51×10^3 M^{-1}.

8 Gaussian calculation and three-dimensional coordinates of C4NP and PPi

The binding of C4NP and PPi were examined by computational calculations at HF/6-31g(d) levels by using Gaussian 09.

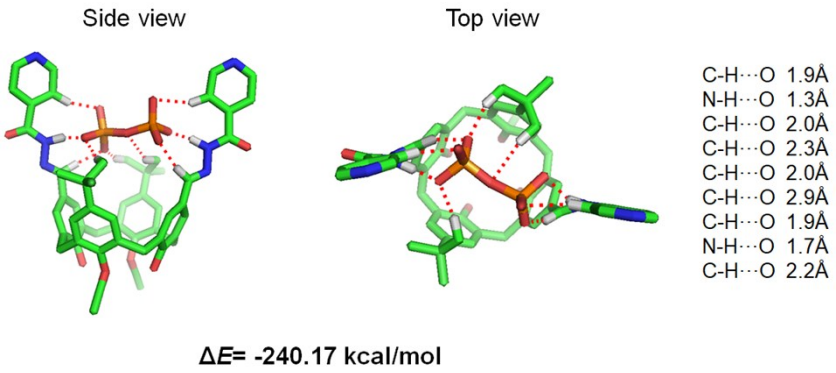

Figure S16. Energy-minimized complex of C4NP with PPi, optimized at the HF/6–31G(d) level. This result shows that C4NP can strongly bind PPi through multiple hydrogen bonds.

Computational model of C4NP binding PPi

%chk=C4NP+PPi.chk

%mem=14GB

%nprocshared=8

opt hf/6-31g(d) geom=connectivity

C4NP+PPi

-4 1

Cartesian Co-ordinates (XYZ format)

O	4.75356900	-2.28764000	1.84748500
C	-0.80212000	-2.52363300	5.10549400
C	-1.50981700	-1.73587700	2.80043800
C	-0.74815500	-0.09408600	4.47720400
C	-0.78248100	1.51033900	-2.98945800
C	0.15902900	1.81783800	-5.32041400
C	2.84622300	-3.47904100	-1.11389700
O	5.76596200	0.44561800	0.78688400
C	0.48443700	3.56974200	-3.58049400
C	0.40965700	2.05315700	-3.81653800
C	0.92332500	-1.74891400	3.47425800
C	1.25987800	-2.90758300	2.77736300
C	2.51091300	-3.12233400	2.21779900
C	2.10508200	-4.02766000	-0.07145900
C	0.72879300	-4.13457500	-0.21803100
C	0.06713800	-3.61428900	-1.32049500
C	0.83228600	-3.03835800	-2.32136000
C	2.21628100	-2.98049500	-2.25215000
C	2.43957800	2.90878400	1.27872900
C	2.81260400	2.01321600	2.26765800
C	3.93476700	1.20594400	2.14927100
C	4.20361000	0.16934300	3.23340900
C	-0.51921900	-1.52449800	3.96327500
C	3.24299200	2.99603400	0.15475500
C	3.46701000	-2.14279800	2.43851200
C	2.77917800	1.98665900	-2.80857700
O	4.21253100	-3.43986700	-0.98711900
C	4.67682800	1.26610500	0.97262400

C	4.32105600	2.14794000	-0.04381200
C	4.90751400	2.04716100	-1.44643600
C	3.90728300	1.31502500	-2.33901200
C	2.73184300	-4.31593400	1.28834700
C	1.93407000	-0.82019500	3.66599600
C	3.21051100	-0.98126900	3.14126000
C	1.71320600	1.33921000	-3.41392500
C	2.98189500	-2.26826900	-3.36187100
C	3.97108000	-0.04056000	-2.58551600
C	1.84181900	-0.03546200	-3.61250100
C	2.95450100	-0.75104200	-3.20844500
C	6.45247500	-3.62036400	3.05713400
C	7.11646200	-0.81290600	-3.53782700
O	5.09231000	-0.77575900	-2.11213000
C	5.62192000	-2.99381200	2.48811500
C	-1.40325500	-3.46061400	-1.34956800
H	0.32460300	2.89862400	1.74790400
H	-1.79815800	-2.52651100	-1.75009200
C	1.09558000	3.54574900	1.31909100
N	0.91322000	4.65848600	0.75652200
N	-0.42517200	5.00073200	0.67008800
C	-0.76431500	6.27562300	0.67924800
O	-0.01760900	7.23692100	0.80901800
C	-2.67431800	7.79883600	0.19190100
C	-3.23025100	5.59704400	0.91922800
C	-4.56401300	5.99693800	0.81694600
C	-2.25822900	6.52650100	0.58788500
C	6.14826500	-0.78876600	-2.85434300
C	-4.01959100	8.07568300	0.13397900
N	-4.96873000	7.19725900	0.44224400
H	-0.12557600	-2.37255100	5.94760900
H	-0.69669700	-3.55465400	4.77578700
H	-1.82031700	-2.39736400	5.46410000
H	-1.35728200	-1.01871400	2.00428300
H	-1.46350800	-2.73701900	2.38458900
H	-2.52638300	-1.57886400	3.14110300
H	-0.64329200	0.63197600	3.67481200

H	-0.10045900	0.15336800	5.32143300
H	-1.77360100	-0.01542900	4.82720600
H	-0.75364900	1.82906700	-1.95470600
H	-0.87203600	0.43279200	-3.01040100
H	-1.70547600	1.90938600	-3.40010900
H	0.98747500	2.18402000	-5.92773700
H	0.01373000	0.76746300	-5.55074100
H	-0.74224500	2.34015000	-5.62745100
H	5.50201600	-0.46080000	0.88437500
H	1.29961800	4.03945200	-4.13337500
H	0.58287000	3.80144000	-2.52729100
H	-0.44443600	4.02304500	-3.91050700
H	0.49940300	-3.64211600	2.60387400
H	0.13215200	-4.54316100	0.57405000
H	0.32463500	-2.59149400	-3.15689100
H	2.17331700	1.90878000	3.12477300
H	5.22572400	-0.18317500	3.18981700
H	4.07617800	0.64615700	4.19981100
H	2.93403500	3.66759900	-0.62148200
H	2.71733900	3.03977600	-2.62735900
H	4.52662500	-2.55597800	-1.12684600
H	5.86433100	1.54775100	-1.43183500
H	5.06101900	3.04526800	-1.84552000
H	3.78357300	-4.54294600	1.19110400
H	2.24910200	-5.18506200	1.72361500
H	1.71624300	0.09086800	4.18395500
H	3.99972100	-2.63215800	-3.41586200
H	2.51405700	-2.51388600	-4.30928000
H	1.02763900	-0.57442900	-4.05647700
H	7.19870500	-4.13166600	3.59884700
H	7.95935200	-0.81807700	-4.16978000
H	-1.94026400	8.54320700	-0.05149600
H	-5.32649800	5.27654100	1.05534200
H	-3.03904900	4.58080500	1.25591400
H	-4.36156900	9.05429500	-0.17290500
N	-2.15128500	-4.33740800	-0.83612700
N	-3.46227500	-3.91988500	-0.77189900

C	-4.43258200	-4.82194700	-0.77687200
O	-4.28262200	-6.02492100	-0.92839900
C	-6.23039300	-2.96159200	-0.55138500
C	-6.87536400	-5.24670600	-0.68747000
C	-8.18764800	-4.84531500	-0.61148800
C	-5.85568100	-4.28993600	-0.65648300
C	-7.59718100	-2.67882100	-0.48214400
N	-8.56547600	-3.57577700	-0.51067700
H	-5.54261800	-2.13154300	-0.49126600
H	-8.98372400	-5.57658500	-0.63568100
H	-7.88827300	-1.64684800	-0.39983900
H	-1.04415200	4.13817200	0.33374800
H	-3.59204300	-2.90923500	-0.51354800
H	-6.61577500	-6.28651900	-0.77324500
P	-3.56003100	-0.47172600	-0.50898100
O	-2.88944500	-1.02465800	-1.76067200
O	-3.48898100	-1.57399900	0.55238200
O	-2.59774100	0.73796200	0.02979100
O	-4.96260000	0.03003600	-0.71992900
P	-2.14843100	2.01034700	0.90780400
O	-1.48850700	2.96365800	-0.13101000
O	-3.34285700	2.68573100	1.53339900
O	-1.08129500	1.55220600	1.89811900

9 Surface charge density (σ) measurement of nanochannels through Electroosmotic Flow (EOF) tests [S6, S7]

The rate of EOF was investigated by measuring the flux of a neutral probe molecule (phenol) across the membrane. A PI membrane which contains multiple nanochannels (channel density ~10^7 per cm^2) was mounted in the home-made cell. The feed half-cell was filled with 10 mM phenol in 10 mM phosphate buffer, pH 7.38, and the permeate half-cell was filled with buffer. EOF was driven from feed to permeate by using a Pt electrode in each half-cell solution to pass a fixed voltage of 2 V through the membrane. Because the nanochannel surfaces have excess negative charge, EOF is in the direction of cation migration. For this reason, the cathode was in the permeate solution for all EOF experiments, as shown in Figure S17.

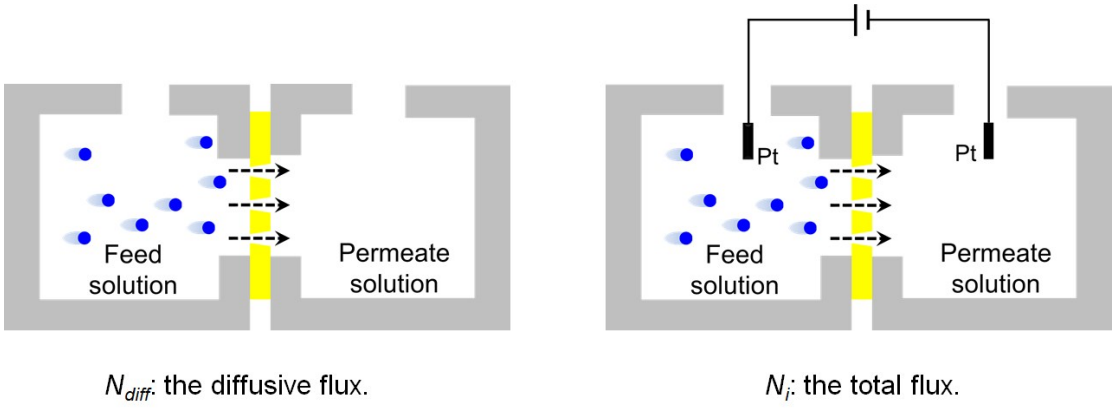

Figure S17. The experimental equipment of phenol transport measurements.

The electroosmotic velocity was obtained by spectrophotometrically measuring the flux of phenol across the membrane. This was accomplished by periodically measuring the fluorescence emission of the phenol in the permeate solution and making plots of moles of phenol transport vs time. The slope of this line is proportional to the flux of phenol across the membrane. When transport is assisted by EOF, the total flux, N_i, has both diffusive and electroosmotic contributions. The diffusive flux, N_{diff}, was obtained independently by doing an analogous experiment in the absence of current.

$$E = \frac{N_i}{N_{diff}} \qquad Formula\ (1)$$

$$E = \frac{Pe}{1 - \exp(-Pe)} \qquad Formula\ (2)$$

$$V_{eof} = Pe \times \frac{D}{L} = -\varepsilon^{\zeta} \times J_{app} \times \frac{\rho}{\eta} \qquad Formula\ (3)$$

$$\sigma = \varepsilon \times \frac{\zeta}{k^{-1}} \qquad Formula\ (4)$$

N_i and N_{diff} were then used to calculate the enhancement factor, E (Formula 1), which was used to calculate the Peclet number, Pe (Formula 2). Pe is related to electroosmotic velocity, V_{eof}, via Formula 3 (L is the membrane thickness and D is the diffusion coefficient for phenol, L=12 μm, D=8.9×10^{-6} cm^{-2}s^{-1}; ε and η are the permittivity and viscosity of the solution, respectively, ε=6.95×10^{-10} C^{2}J^{-1}m^{-1}, η=0.890 cp; ρ is the resistivity of the electrolyte within the nanochannel, ρ=2.23 KΩ; J_{app} is the constant applied current density; ζ is the zeta potential of the nanochannel wall). We may extract the ζ and then surface charge density (σ) values can be estimated from the Gouy-Chapman equation (κ^{-1} is the effective thickness of the electrical double layer, κ^{-1}=(9.61×10^{-9})(z^{2}c) $^{-1/2}$) (Formula 4). Hence, the surface charge density can be calculated from above formulas.

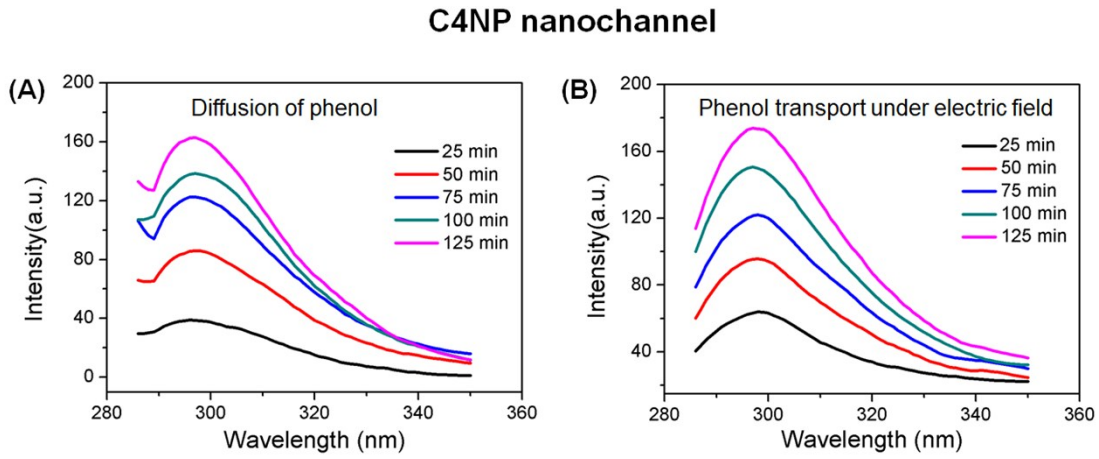

Figure S18. The fluorescence spectra of phenol transport through C4NP nanochannel (A) without and (B) with an external electric field.

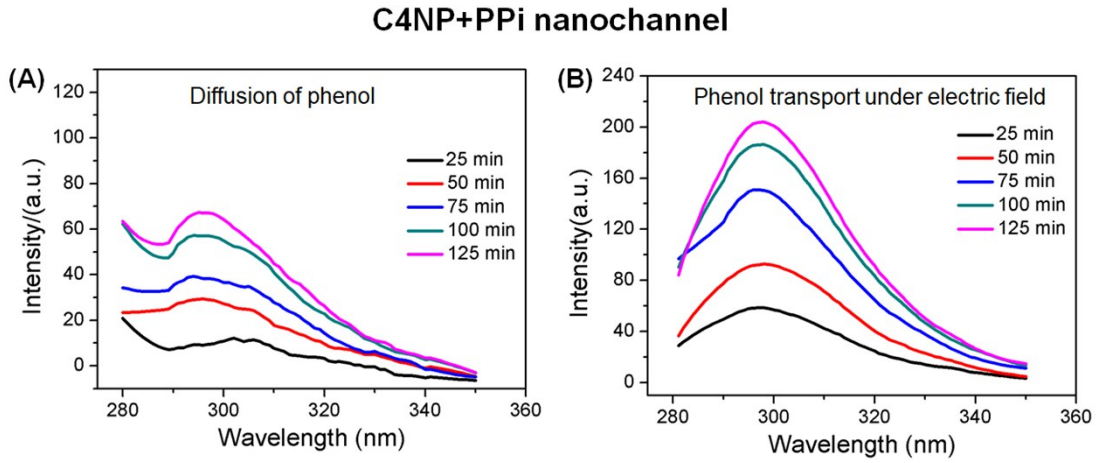

Figure S19. The fluorescence spectra of phenol transport through C4NP+PPi nanochannel (A) without and (B) with an external electric field.

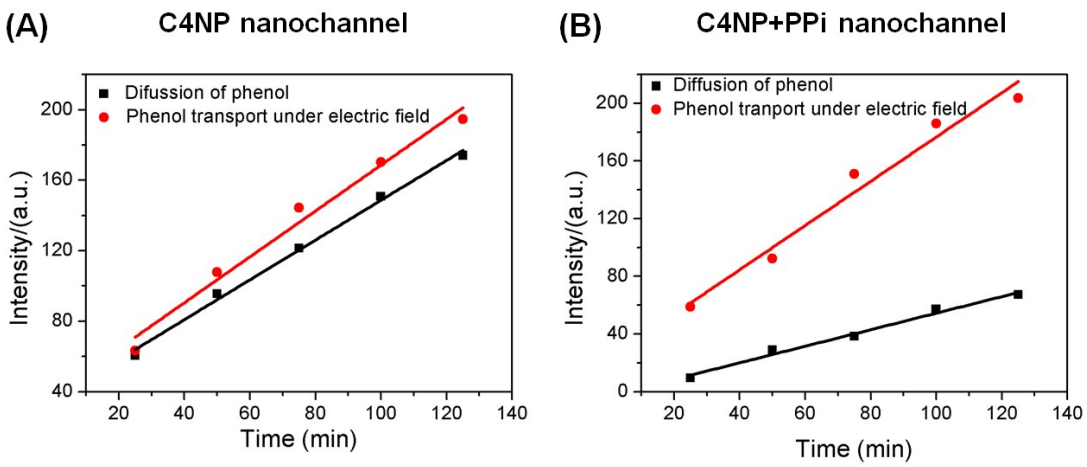

Figure S20. The plotted curve of the fluorescence intensity changing with time.

According to Figure S20, the enhancement factors of C4NP nanochannel and C4NP+PPi nanochannel were 1.15 and 2.67, respectively. So the surface charge densities could be calculated, which are shown in Table S2.

Table S2. The inner surface charge density (σ) of the nanochannel

	J_{app} (mA cm^{-2})	V_{eof} (cm s^{-1})	ξ (mV)	σ (e nm^{-2})
C4NP nanochannel	0.065	2.26×10^{-3}	-0.726	-0.018
C4NP+PPi nanochannel	0.195	1.81×10^{-3}	-0.949	-0.048

10 The numerical simulation of ion concentration distribution

The Finite-element computations were performed on the Poisson and Nernst−Planck equations using COMSOL Multiphysics 5.3. [S8] The equations are shown below:

$$J_i = D_i\left(\nabla c_i + \frac{z_i F c_i}{RT}\nabla\varphi\right) + uc_i \qquad \text{Formula (5)}$$

$$\nabla^2\varphi = -\frac{F}{\varepsilon}\sum z_i c_i \qquad \text{Formula (6)}$$

$$\nabla \cdot J_i = 0 \qquad \text{Formula (7)}$$

Formula 5 is the Nernst–Planck equation that describes the transport property of a charged nanochannel. The electric potential and ionic concentration can be characterized by Formula 6. Besides, the flux should satisfy the time-independent continuity when the system reaches a stationary regime (Formula 5). The physical quantities J_i, D_i, c_i, φ, u, R, F, T, and ε refer to the ionic flux, diffusion coefficient, ion concentration, electrical potential, fluid velocity, universal gas constant, Faraday constant, absolute temperature, and dielectric constant of the electrolyte solutions, respectively. The coupled equations can be solved by assuming appropriate boundary conditions. The boundary condition for potential φ on the channel wall is Formula 8; and the ionic flux has zero normal components at boundaries (Formula 9), where σ represents the surface charge density and is given by the EOF experiment.

$$\underset{n}{\rightarrow} \cdot \nabla\varphi = -\frac{\sigma}{\varepsilon} \qquad \text{Formula (8)}$$

$$\underset{n}{\rightarrow} \cdot J_i = 0 \qquad \text{Formula (9)}$$

Electrolyte solution was 0.1 M KCl, and the diffusion coefficients of K^+ and Cl^- were set as 1.957×10^{-9} m^2 s^{-1} and 2.032×10^{-9} m^2 s^{-1}, respectively. The simulated model is

shown in **Figure S21**.

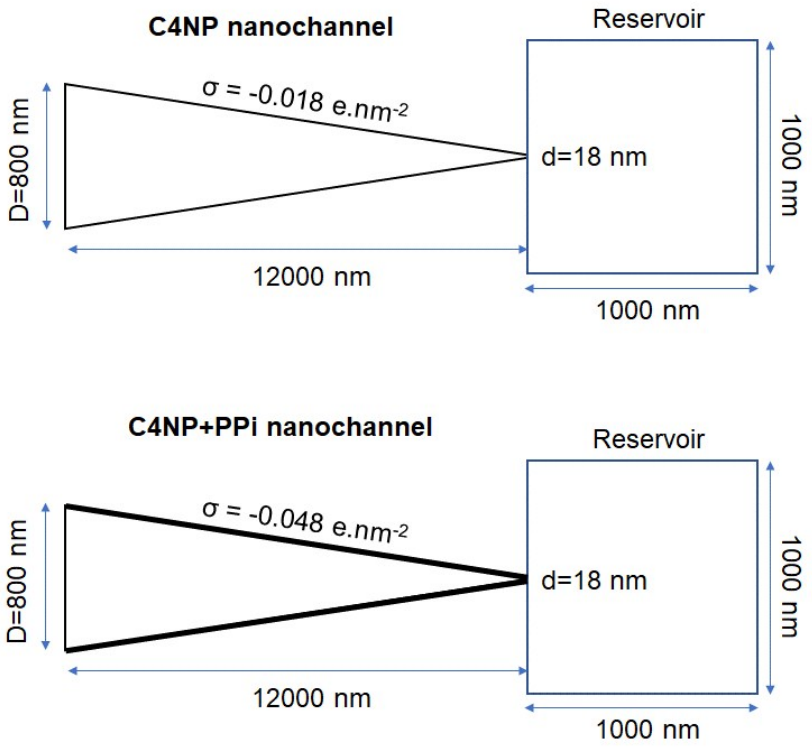

Figure S21. The model of numerical simulation about C4NP nanochannel and C4NP+PPi nanochannel (length and width are not to scale). As shown in the Figure, the model of nanochannel is set to 12000 nm (length), 800 nm (base side), and 18 nm (tip side). The reservoirs with a width of 1000 nm and a height of 1000 nm. The surface charge density of C4NP nanochannel (-0.018 e nm^{-2}) and C4NP+PPi nanochannel (-0.048 e nm^{-2}) are measured by EOF experiments. Applying -2V potential at the base side as a driving force to demonstrate the ion behavior under experimental conditions.

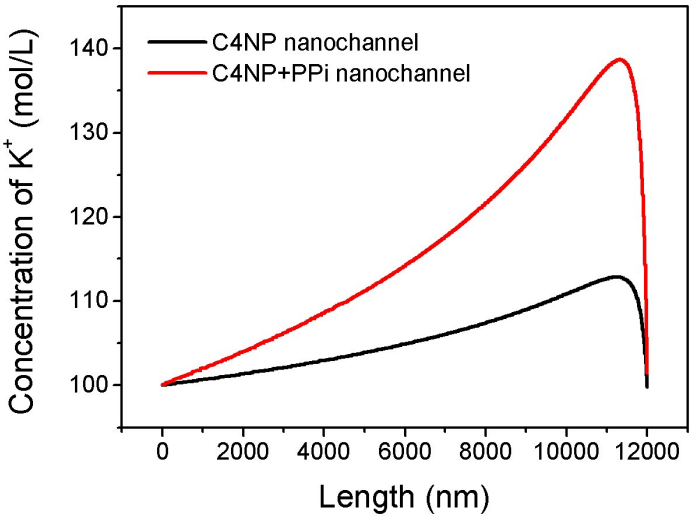

Figure S22. The numerical simulation of ion concentration (total of K^+) distribution in the C4NP nanochannel and C4NP+PPi nanochannel (at −2 V, with 0.1 M KCl).

11 References

S1. Y. Sun, Y. Mei, J. Quan, X. Xiao, L. Zhang, D. Tian, H. Li. *Chem. Commun.*, **2016**, *52*, 14416−14418.

S2. Z. Siwy, E. Heins, C. C. Harrell, P. Kohli, C. R. Martin, *J. Am. Chem. Soc.*, **2004**, *126*, 10850–10851.

S3. G. Nie, Y. Sun, F. Zhang, M. Song, D. Tian, L. Jiang, H. Li, *Chem. Sci.*, **2015**, *6*, 5859–5865.

S4. Y. Sun, F. Zhang, J. Quan, F. Zhu, W. Hong, J. Ma, H. Pang, Y. Sun, D. Tian, H. Li, *Nat. Commun.*, **2018**, *9*, 2617.

S5. Y. Ma, X. Ji, F. Xiang, X. Chi, C. Han, J. He, Z. Abliz, W. Chen, F. Huang, *Chem. Commun.*, **2011**, *47*, 12340–12342.

S6. S. A. Miller, V. Y. Young, C. R. Martin, *J. Am. Chem. Soc.*, **2001**, *123*, 12335–12342.

S7. P. Jin, H. Mukaibo, L. P. Horne, G. W. Bishop and C. R. Martin, *J. Am. Chem. Soc.*, **2010**, *132*, 2118–2119.

S8. K. Xiao, G. Xie, Z. Zhang, X. Kong, Q. Liu, P. Li, L. Wen, L. Jiang, *Adv. Mater.*, **2016**, *28*, 3345–3350.